A mechanical metamaterial made from a DNA hydrogel

Jong Bum Lee^{1,2†}, Songming Peng^{1†}, Dayong Yang¹, Young Hoon Roh¹, Hisakage Funabashi^{1,3}, Nokyoung Park^{1,4}, Edward J. Rice¹, Liwei Chen⁵, Rong Long¹, Mingming Wu¹ and Dan Luo^{1*}

Metamaterials are artificial substances that are structurally engineered to have properties not typically found in nature. To date, almost all metamaterials have been made from inorganic materials such as silicon and copper^{1,2}, which have unusual electromagnetic or acoustic properties¹⁻⁵ that allow them to be used, for example, as invisible cloaks⁶⁻⁹, superlenses¹⁰⁻¹² or super absorbers for sound¹³. Here, we show that metamaterials with unusual mechanical properties can be prepared using DNA as a building block. We used a polymerase enzyme to elongate DNA chains and weave them noncovalently into a hydrogel. The resulting material, which we term a meta-hydrogel, has liquid-like properties when taken out of water and solid-like properties when in water. Moreover, upon the addition of water, and after complete deformation, the hydrogel can be made to return to its original shape. The meta-hydrogel has a hierarchical internal structure and, as an example of its potential applications, we use it to create an electric circuit that uses water as a switch.

We have previously developed bulk-scale, DNA-based materials^{14–20} that can be used in practical applications such as multiplexed diagnosis^{17,19,21}, vaccine and drug delivery^{22–24} and cell-free protein production²⁰. In particular, we created a hydrogel that was made entirely of DNA and crosslinked by enzymes (T4 ligase)¹⁸. In the present work we take a different approach. Instead of crosslinking DNA chains covalently into a chemical hydrogel (via a ligase), we have elongated DNA chains and woven them noncovalently into a physical hydrogel (via a polymerase). To fabricate our DNA meta-hydrogel, we chose a special polymerase, Φ 29, a bacteria phage polymerase that is capable of DNA chain elongation and displacement, thus amplifying and weaving DNA²⁵. Φ29 uses a single-stranded DNA (ssDNA) as a template to elongate the primer, while at the same time displacing the newly synthesized strands into ssDNA products. Based on Φ 29, we designed a unique combination of two sequential processes: (i) a rolling circle amplification (RCA, or R) followed by (ii) a multi-primed chain amplification (MCA, or M). After running the RCA for x hours followed by the MCA for y hours, a chain reaction was established, resulting in a DNA hydrogel (Fig. 1, Supplementary Fig. S1, Table S1 and Discussion SI). To simplify the notation, we abbreviate our procedures as $\mathbf{R}_{x}\mathbf{M}_{y}$.

The enzymatic processes were monitored by observing the optical density (OD_{600}). For example, when the **R**-process was set at 4 h, the OD increased with the duration of the **M**-process (Supplementary Fig. S2). When the **M**-process reached 16 h ($\mathrm{R}_4\mathrm{M}_{16}$), a totally opaque gel was obtained (Fig. 2a). As expected, this hydrogel showed fluorescence after staining with a DNA-specific dye (GelGreen, Fig. 2b), indicating that the entire hydrogel

was composed of DNA. Rheology data further confirmed that the $\mathbf{R_4M_{16}}$ was a true gel, as the shear-storage modulus (G') was constantly higher than the shear-loss modulus (G'') over the entire frequency range (Fig. 2c). On the other hand, when the **R**-process continued alone for 20 h ($\mathbf{R_{20}M_0}$), a viscous solution was produced (Supplementary Fig. S2), and there were no detectable signals in the rheometer, proving that the $\mathbf{R_{20}M_0}$ was just a liquid. We further tested the gel formation by varying the combinations of x and y and found that a minimum of x=2 h and y=16 h was required to create a DNA hydrogel (Supplementary Table S2). As expected²⁶, the hydrogel in solution melted at 85 °C due to denaturing of the DNA strands (Supplementary Fig. S3).

Unexpectedly, we discovered unusual metaproperties in our DNA hydrogel—it had either liquid-like or solid-like properties depending on the physical environment. When the gel was taken out of water it became a 'liquid' that flowed freely in a tube (Fig. 3a), and when placed in differently shaped containers conformed to the shape of the containers (Fig. 3b). However, when put back into water, it metamorphosed into a solid gel. We emphasize that although the hydrogel behaved like a liquid, it was still a gel. Surprisingly, it always returned rapidly to its original shape in water, regardless of how many different shapes it had adopted while in the liquid-like state. To further investigate this unusual property, we first formed R₄M₁₆ meta-hydrogel in moulds with defined geometries in the shape of the letters D, N and A (Fig. 3c). After removing water, each hydrogel behaved like a liquid by conforming to the shape of the vial (Fig. 3d). However, when the water was reintroduced, the hydrogels returned to their original shapes (D, N and A) within 15 s (Fig. 3e-f). The entire event was captured by video (Supplementary Movie S1). These liquid-solid transition and returning-to-original-shape processes can be repeated as many times as required. Furthermore, the hydrogel can be remoulded into new shapes upon heating the gel above its denaturing temperature (Supplementary Fig. S4). These results therefore clearly demonstrate the fabrication of a novel organic-based metamaterial.

Unlike conventional hydrogels, which have amorphous internal structures 18,20,27 , our $R_4M_{16}\,$ meta-hydrogel has a hierarchical internal structure, as revealed by field-emission scanning electron microscopy (FESEM). At the microscale, the densely packed DNA microstructures are in the shape of a bird nest (Fig. 4a,b). These nest structures are of uniform size and woven together by DNA. Within each microstructure, the internal porous nanostructures were observed by cutting the DNA nest in half using a focused ion beam (Fig. 4c). To the best of our knowledge, this hierarchical structural organization has not previously been seen in hydrogels, and may contribute to its metaproperties.

¹Department of Biological and Environmental Engineering, Cornell University, Ithaca, New York 14853, USA, ²Department of Chemical Engineering, University of Seoul, Seoul 130-743, South Korea, ³Institute for Sustainable Sciences and Development, Hiroshima University, Higashi-Hiroshima City 739-8511, Japan, ⁴Frontier Research Lab., Samsung Advanced Institute of Technology 449-712, South Korea, ⁵Suzhou Institute of Nano-Tech and Nano-Bionics, Chinese Academy of Sciences, Suzhou 215123, China; [†]These authors contributed equally to this work. *e-mail: dan.luo@cornell.edu

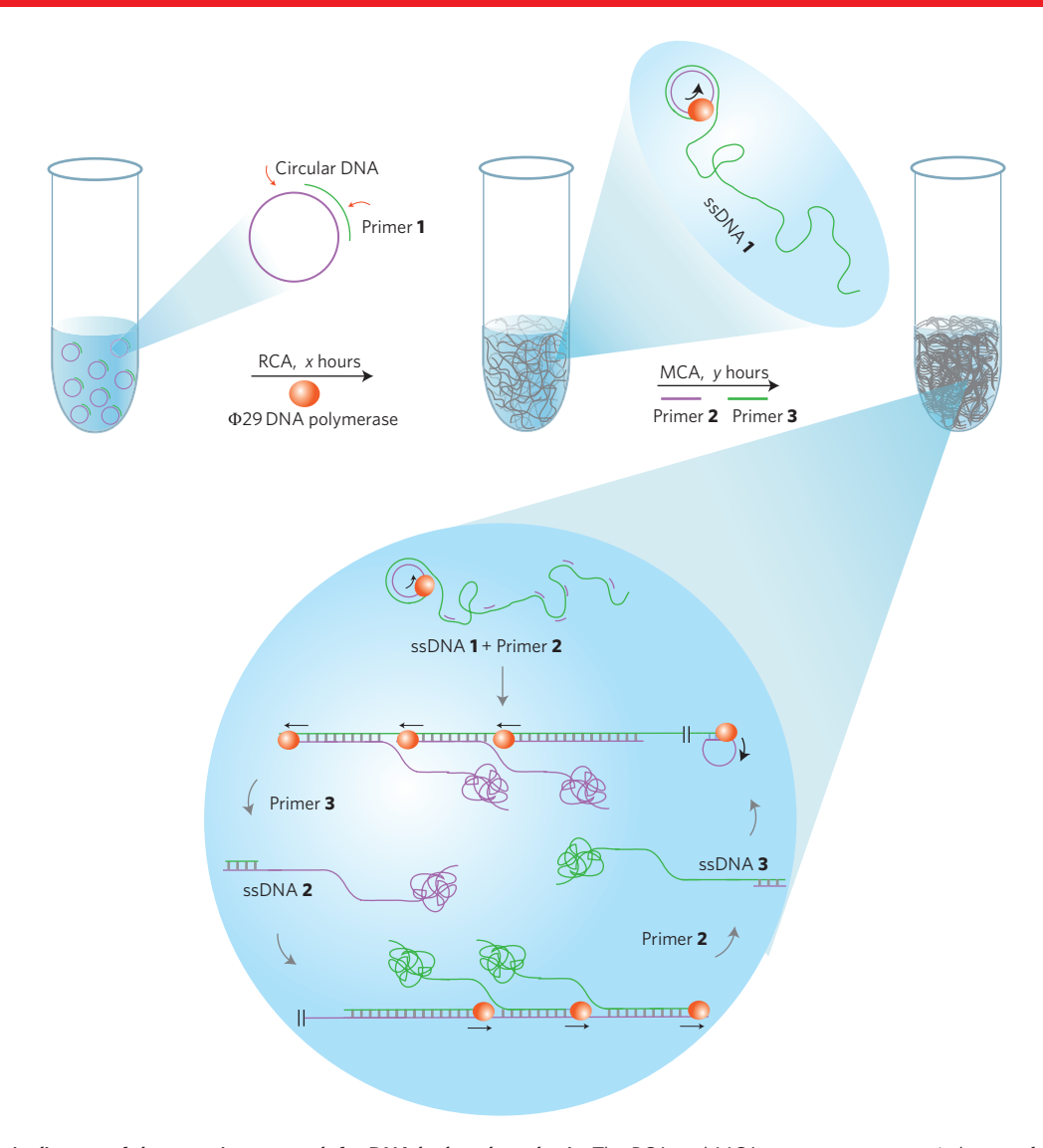


Figure 1 | Schematic diagram of the stepwise approach for DNA hydrogel synthesis. The RCA and MCA processes were carried out as follows. (i) In the R process, a circular ssDNA template was first produced (Supplementary Fig. S1 and Table S1), then a complementary primer for RCA (Primer 1) was added to produce elongated ssDNA products (termed ssDNA 1: tandem repeats of the sequences complementary to the original circular ssDNA template). (ii) In the M process, after RCA, we added two additional primers (Primer 2 and Primer 3) for subsequent chain amplification. Primer 2 was elongated to generate ssDNA 2 (complementary to ssDNA-1). Primer 3 was used to create ssDNA 3 (complementary to ssDNA 2; thus ssDNA 3 and ssDNA 1 had exactly the same sequences). Primer 2 was also therefore able to produce more ssDNA 2 using newly synthesized ssDNA 3 as templates, leading to chain amplification.

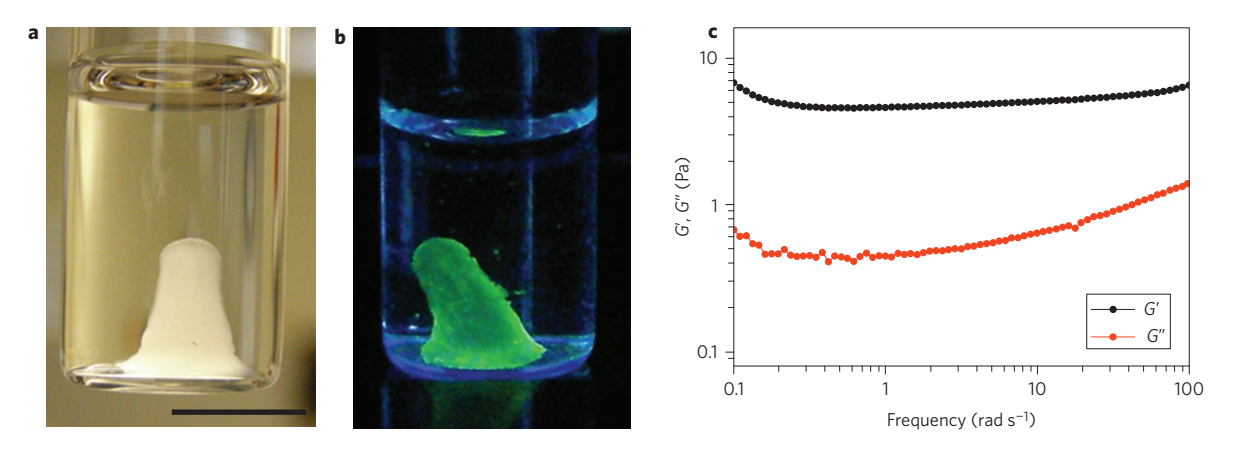


Figure 2 | Characterization of the R_4M_{16} DNA hydrogel. **a**, Photograph of the R_4M_{16} hydrogel. Scale bar, 10 mm. **b**, Hydrogels stained with GelGreen, a DNA-specific dye. **c**, Storage-loss (G') and shear-loss (G'') moduli of R_4M_{16} hydrogel from a rheometer measurement.

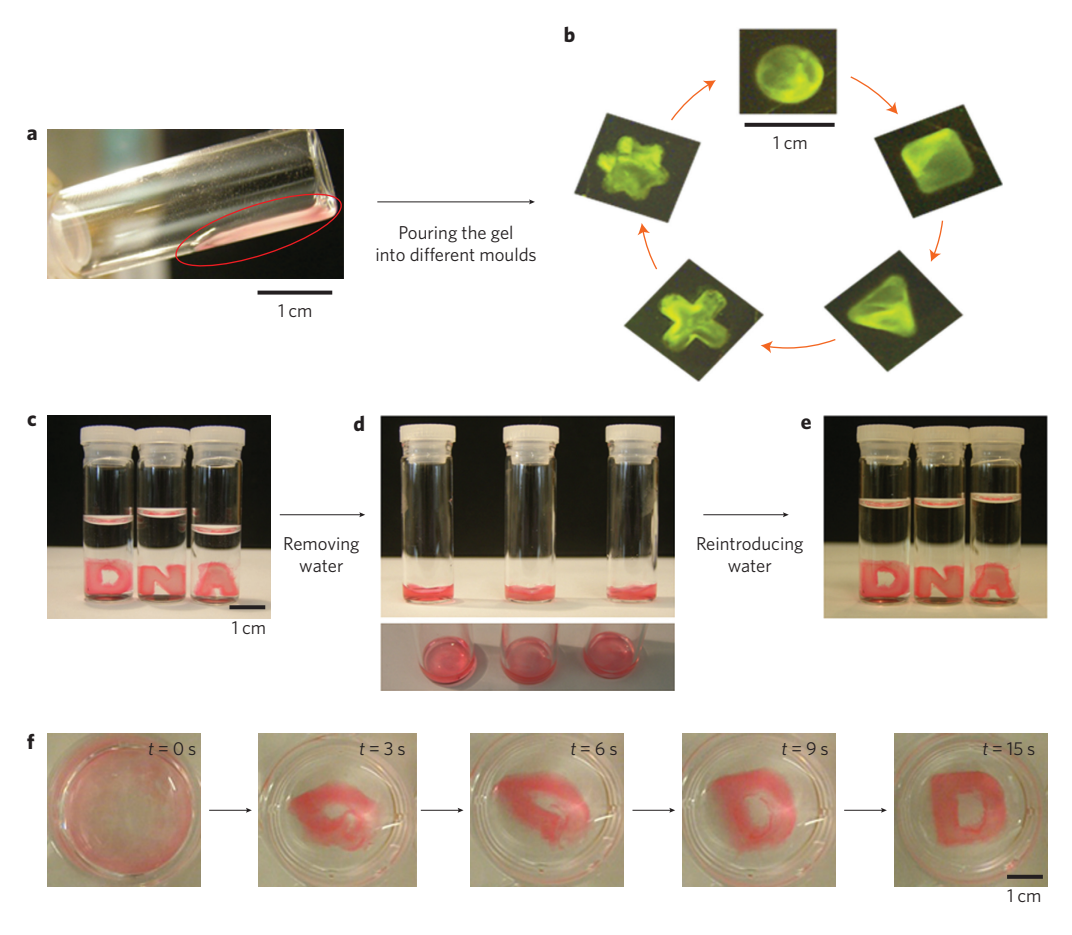


Figure 3 | Liquid- and solid-like properties of the R_4M_{16} hydrogel. **a**, When out of water, the hydrogel flows freely in the tube. **b**, When poured into differently shaped containers consecutively and repeatedly (from circular, to square, to triangular, to X-shaped, to star-shaped, then back to circular), the hydrogel conforms to the shape of the container, just like a liquid. The gel was stained with GelGreen. **c**, D-, N- and A-shaped hydrogel was successfully formed and its solid-like property tested by removing and replacing water. **d-f**, Series of photographs showing the process of DNA hydrogel returning to its original shape after reintroducing water at 25 °C: the gels begin to metamorphose within the first 3 s (t = 0-3 s). The gel continues to transform back to its original shape, gradually and smoothly (t = 3-9 s). The final D shape is restored within 15 s (t = 15 s).

We further selectively tuned the hierarchical microstructures by separately changing the reaction times of **R** and **M**. More specifically, by increasing the **M** reaction time from 1 h to 16 h while keeping **R** constant at 4 h (that is, R_4M_1 , R_4M_3 , R_4M_6 and R_4M_{16}), we produced more developed DNA bird nests (Supplementary Fig. S5a–d). The diameter of the bird nest increased from $\sim\!0.3~\mu\mathrm{m}$ in R_4M_1 to $\sim\!1.6~\mu\mathrm{m}$ in R_4M_{16} . On the other hand, by lengthening the **R** process from 0 h to 8 h while keeping **M** constant at 16 h (that is, R_0M_{16} , R_1M_{16} , R_2M_{16} , R_4M_{16} and R_8M_{16}), we obtained more densely populated bird nests of almost identical size (Fig. 4d–h, the number of bird nests were from $10\pm2/100~\mu\mathrm{m}^2$ in R_0M_{16} to $35\pm5/100~\mu\mathrm{m}^2$ in R_8M_{16}). We emphasize that these differently tuned hierarchical internal structures (in terms of size and density of the DNA bird nests) were accomplished by designing and controlling the enzymatic reactions of R_xM_v .

Through the morphology studies we discovered that the two enzymatic reactions **R** and **M** determine the internal hierarchical structures, which in turn leads to the observed metaproperties. Indeed, the metaproperties are only found when x = 2-8 h and $y \ge 16$ h (Supplementary Table S2). Although the complete mechanism for the metaproperties is still subject to investigation, we propose the following theory. From an enzymatic perspective and based on the well-known characteristics of Φ 29 and the design of our unique primers, the **R** process first generates a large number of long tandem ssDNA, which in turn serve as templates for the **M** process, the products of which are both long ssDNA and

dsDNA. As revealed in the morphology studies, these DNA strands are woven together into bird nests as well as linear bundles by enzymatic processes. From a physics aspect, we attribute the liquid- and solid-like properties to the ultralow elastic modulus of our DNA hydrogel. When a hydrogel is exposed to air, the gel is deformed by surface tension and gravity, which is energetically penalized by the strain energy due to elastic deformation. Such deformation due to surface tension and gravity is negligible for most solids as the strain energy penalty is too high because of the large modulus E (ranging from kPa to GPa) 18,28,29. However, because our DNA hydrogel is extremely soft ($E \approx 10$ Pa; Fig. 2c, Supplementary Fig. S6), both the surface energy and the gravitational energy completely outweigh the strain energy. As a result, the gel shape is primarily determined by surface tension and gravity when exposed to air and it behaves like a liquid. When the gel is immersed in water, on the other hand, the surface tension is practically zero, and buoyancy forces cancel the gravity. Thus, the hydrogel behaves like a solid and retains its original shape. The whole process is illustrated in Supplementary Fig. S7, and more theoretical calculations are deduced in Supplementary Discussion SII.

A variety of applications can be envisioned using either or both liquid-like and solid-like properties of our meta-gels. As an example, we designed a DNA-meta-hydrogel-based electric circuit that uses water as a switch (Fig. 5). When the surrounding water was removed, the DNA meta-hydrogel (doped with 10 nm gold

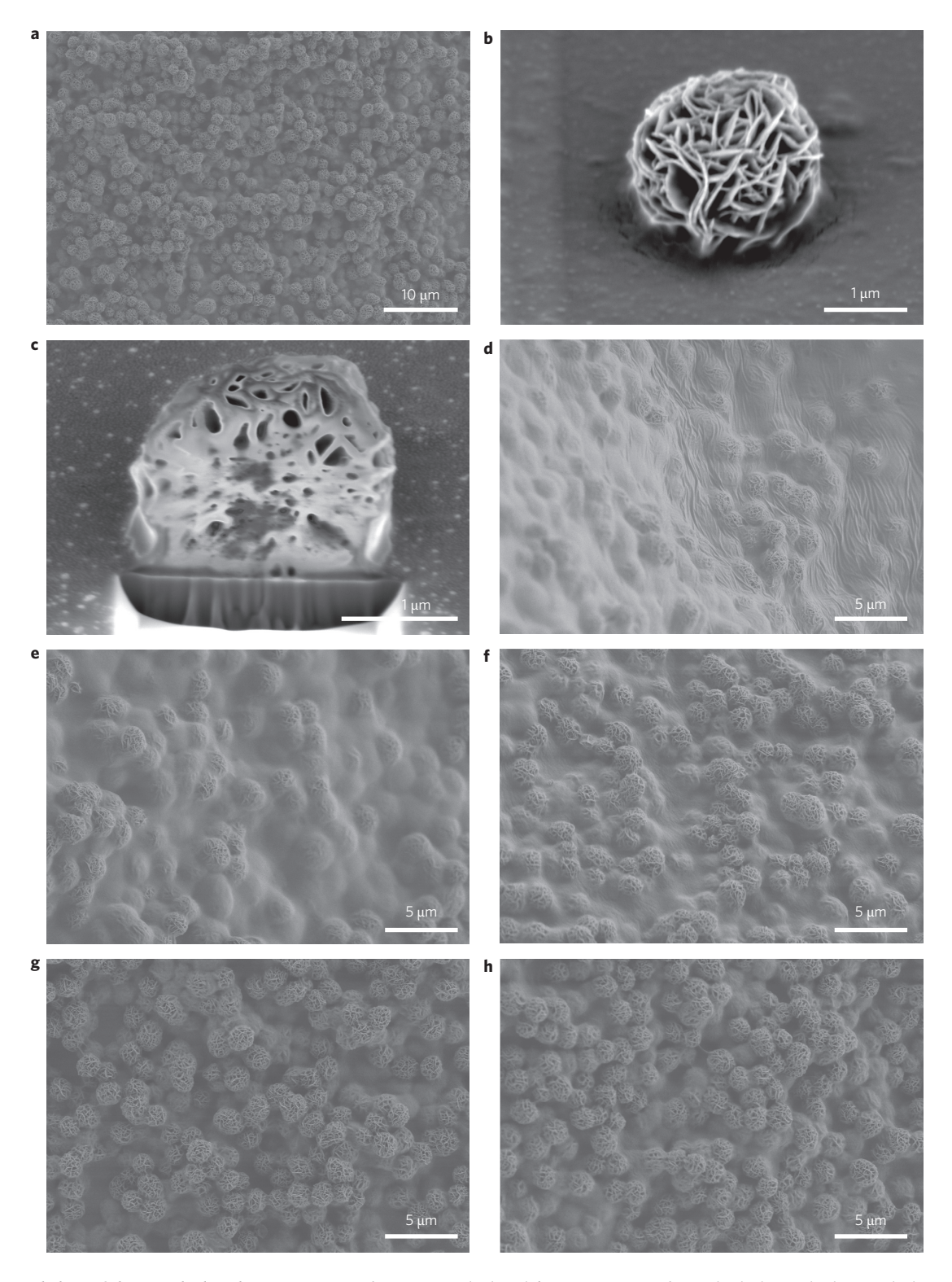


Figure 4 | Morphology of the DNA hydrogel. a, SEM images of $\mathbf{R}_4\mathbf{M}_{16}$ DNA hydrogel. **b,c**, SEM images of an individual DNA bird nest, which was isolated (**b**) then cut with a focused ion beam (**c**). **d-h**, SEM images for different RCA times: $\mathbf{R}_0\mathbf{M}_{16}$ (**d**), $\mathbf{R}_1\mathbf{M}_{16}$ (**e**), $\mathbf{R}_2\mathbf{M}_{16}$ (**f**), $\mathbf{R}_4\mathbf{M}_{16}$ (**g**) and $\mathbf{R}_8\mathbf{M}_{16}$ (**h**).

nanoparticles to provide electric conductivity) became 'liquid-like' and thus conformed to the shape of the channel linking the two electrodes together. As a result, the circuit was turned on (Fig. 5, 'ON'). By simply adding water to the meta-hydrogel, it once again became 'solid-like' and returned to its original, shorter shape, thereby causing the gel to rapidly move away from the electrode and completely shut off the current (Fig. 5, 'OFF'). This simple demonstration shows one application that takes advantage of the

metaproperties of our meta-hydrogel, but it can also be applied to biomedical applications such as controlled drug release for multiple drugs (Supplementary Fig. S8). More applications in other fields are also being explored.

In conclusion, we have designed and programmed two enzyme processes to achieve a novel DNA meta-hydrogel. These specifically designed enzymatic processes generate a striking internal morphology with hierarchical structure and confer our DNA hydrogel

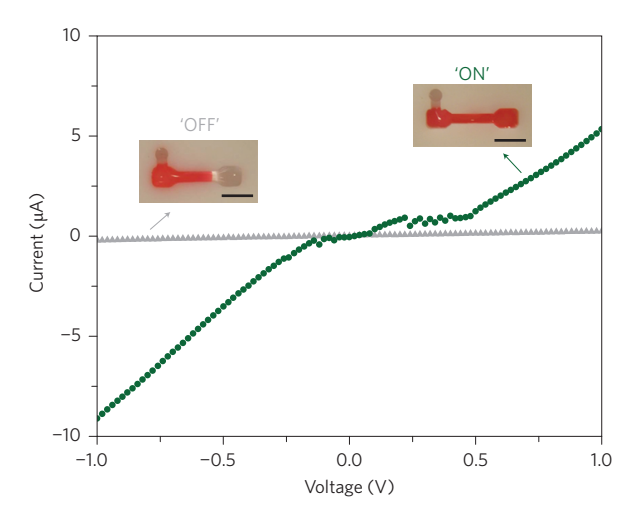


Figure 5 | Electric circuit switch formed using the liquid- and solid-like properties of DNA meta-hydrogel. When the DNA meta-hydrogel (containing 10 nm gold nanoparticles) has liquid-like properties, the circuit can be covered by the gel (green circles, 'ON'). By simply adding water, the gel metamorphoses to its original shape, which is shorter, resulting in the gel rapidly moving away (within seconds) from the electrode and completely shutting off the current (grey triangles, 'OFF'). Scale bars (insets), 5 mm.

with metaproperties. The DNA meta-hydrogel notably expands the metamaterial repertoire and has potential for real-world applications, including drug release, cell therapy, electric switches and flexible circuits.

Received 10 September 2012; accepted 31 October 2012; published online 2 December 2012

References

- Shelby, R. A., Smith, D. R. & Schultz, S. Experimental verification of a negative index of refraction. *Science* 292, 77–79 (2001).
- Liu, Y. M. & Zhang, X. Metamaterials: a new frontier of science and technology. Chem. Soc. Rev. 40, 2494–2507 (2011).
- 3. Pendry, J. B., Holden, A. J., Stewart, W. J. & Youngs, I. Extremely low frequency plasmons in metallic mesostructures. *Phys. Rev. Lett.* **76**, 4773–4776 (1996).
- Smith, D. R., Padilla, W. J., Vier, D. C., Nemat-Nasser, S. C. & Schultz, S. Composite medium with simultaneously negative permeability and permittivity. *Phys. Rev. Lett.* 84, 4184–4187 (2000).
- Smith, D. R., Pendry, J. B. & Wiltshire, M. C. K. Metamaterials and negative refractive index. Science 305, 788–792 (2004).
- Alu, A. & Engheta, N. Achieving transparency with plasmonic and metamaterial coatings. *Phys. Rev. E* 72, 016623 (2005).
- Schurig, D. et al. Metamaterial electromagnetic cloak at microwave frequencies. Science 314, 977–980 (2006).
- 8. Liu, R. et al. Broadband ground-plane cloak. Science 323, 366–369 (2009).
- Fridman, M., Farsi, A., Okawachi, Y. & Gaeta, A. L. Demonstration of temporal cloaking. *Nature* 481, 62–65 (2012).
- Grbic, A. & Eleftheriades, G. V. Overcoming the diffraction limit with a planar left-handed transmission-line lens. *Phys. Rev. Lett.* 92, 117403 (2004).
- Fang, N., Lee, H., Sun, C. & Zhang, X. Sub-diffraction-limited optical imaging with a silver superlens. Science 308, 534–537 (2005).
- Rogers, E. T. F. et al. A super-oscillatory lens optical microscope for subwavelength imaging. Nature Mater. 11, 432–435 (2012).

- 13. Mei, J. et al. Dark acoustic metamaterials as super absorbers for low-frequency sound. Nature Commun. 3, 756 (2012).
- Roh, Y. H., Ruiz, R. C. H., Peng, S. M., Lee, J. B. & Luo, D. Engineering DNA-based functional materials. *Chem. Soc. Rev.* 40, 5730–5744 (2011).
- Tan, S. J., Campolongo, M. J., Luo, D. & Cheng, W. L. Building plasmonic nanostructures with DNA. *Nature Nanotech.* 6, 268–276 (2011).
- Li, Y. G. et al. Controlled assembly of dendrimer-like DNA. Nature Mater. 3, 38–42 (2004).
- Li, Y. G., Cu, Y. T. H. & Luo, D. Multiplexed detection of pathogen DNA with DNA-based fluorescence nanobarcodes. *Nature Biotechnol.* 23, 885–889 (2005).
- Um, S. H. et al. Enzyme-catalysed assembly of DNA hydrogel. Nature Mater. 5, 797–801 (2006).
- Lee, J. B. et al. Multifunctional nanoarchitectures from DNA-based ABC monomers. Nature Nanotech. 4, 430–436 (2009).
- Park, N., Um, S. H., Funabashi, H., Xu, J. F. & Luo, D. A cell-free protein-producing gel. *Nature Mater.* 8, 432–437 (2009).
- Feng, X. L. et al. Fluorescence logic-signal-based multiplex detection of nucleases with the assembly of a cationic conjugated polymer and branched DNA. Angew. Chem. Int. Ed. 48, 5316–5321 (2009).
- Sil, D., Lee, J. B., Luo, D., Holowka, D. & Baird, B. Trivalent ligands with rigid DNA spacers reveal structural requirements for IgE receptor signaling in RBL mast cells. ACS Chem. Biol. 2, 674–684 (2007).
- Cheng, E. J. et al. A pH-triggered, fast-responding DNA hydrogel. Angew. Chem. Int. Ed. 48, 7660–7663 (2009).
- Rattanakiat, S., Nishikawa, M., Funabashi, H., Luo, D. & Takakura, Y. The assembly of a short linear natural cytosine–phosphate–guanine DNA into dendritic structures and its effect on immunostimulatory activity. *Biomaterials* 30, 5701–5706 (2009).
- Dean, F. B., Nelson, J. R., Giesler, T. L. & Lasken, R. S. Rapid amplification of plasmid and phage DNA using phi29 DNA polymerase and multiply-primed rolling circle amplification. *Genome Res.* 11, 1095–1099 (2001).
- Lee, J. B., Shai, A. S., Campolongo, M. J., Park, N. & Luo, D. Three-dimensional structure and thermal stability studies of DNA nanostructures by energy transfer spectroscopy. *ChemPhysChem* 11, 2081–2084 (2010).
- Roh, Y. H. et al. Photocrosslinked DNA nanospheres for drug delivery. *Macromol. Rapid Commun.* 31, 1207–1211 (2010).
- Cauich-Rodriguez, J. V., Deb, S. & Smith, R. Effect of cross-linking agents on the dynamic mechanical properties of hydrogel blends of poly(acrylic acid)– poly(vinyl alcohol vinyl acetate). *Biomaterials* 17, 2259–2264 (1996).
- Xing, Y. Z. et al. Self-assembled DNA hydrogels with designable thermal and enzymatic responsiveness. Adv. Mater. 23, 1117–1121 (2011).

Acknowledgements

The authors thank L. Archer and R. Mallavajula for helping with the mechanical test and C. Hui for insightful discussions. The authors also thank J. March, J. Hunter and T. Walter for proofreading this manuscript and Z. Li for discussions and suggestions. L.C. acknowledges support from the CAS/SAFEA International Partnership Program for Creative Research Teams. The present work was partially supported by grants from the United States Department of Agriculture (USDA) and the Department of Defense (DOD).

Author contributions

J.B.L., S.P. and D.L. designed the experiments. J.B.L., S.P., Y.H.R., H.F., N.P. and E.R. carried out the experiments. J.B.L., S.P., Y.H.R., H.F., D.Y., L.C., R.L., M.W. and D.L. contributed to the data analysis. J.B.L., S.P., Y.H.R., D.Y., R.L. and D.L. wrote the manuscript.

Additional information

Supplementary information is available in the online version of the paper. Reprints and permission information is available online at http://www.nature.com/reprints. Correspondence and requests for materials should be addressed to D.L.

Competing financial interests

The authors declare no competing financial interests.